Selective Azide Oxidation of 1,2-Bis(diphenylphosphino)benzene and Related Ethylenebis(phosphines) to Asymmetric Multifunctional Phosphorus Ligands and Formation of Rhodium(I) Complexes of These Ligands. Structural Characterization of the Prototypical Ligand 1-(((Trimethylsilyl)imino)diphenylphosphorano)-2-(diphenylphosphino)benzene and Its Rhodium(I) Complex: 1-Ph_2P=N($SiMe_3$)C_6H_4-2-(Ph_2P)Rh(CO)Cl

Robert W. Reed, Bernard Santarsiero, and Ronald G. Cavell*

Department of Chemistry, University of Alberta, Edmonton, AB, Canada T6G 2G2

Received November 15, 1995[⊗]

Selective azide mono-oxidation of *o*-bis(phosphines) such as *o*-bis(diphenylphosphino)benzene and other bis(phosphines) with *cis*-substituents on a rigid backbone such as an ethylene structure occurs as the result of the steric control exerted during the azide oxidation (Staudinger) reaction process. The azides used were the trimethylsilyl, 4-cyanotetrafluorophenyl, benzyl, and diphenoxyphosphonyl azides. The prototypical ligand 1-Ph_2P=N($SiMe_3$)-2-(Ph_2P)C_6H_4, **2**, has been structurally characterized. Crystal data for **2**: crystal dimensions, 0.38 × 0.38 × 0.57 mm; space group, monoclinic, $P2_1/c$, (No. 14); a = 11.093(5) Å, b = 14.898(5) Å, c = 18.811(2) Å, β = 102.76(2)°, V = 3031 Å^3, Z = 4. Final R, R_w and GOF values were 0.068, 0.074, and 1.92 respectively. The P=N−$SiMe_3$ angle was wide, 152.7(3)°, and the P=N bond length short (1.529(5) Å) relative to arylated iminophosphoranes but in keeping with the trends for silylated analogs. The iminophosphorane center can be selectively transformed with other agents in a Wittig type reaction converting the azides to the monooxide, monosulfide, etc. The iminophosphoranophosphines are also good complexing agents and the Rh(I) complex derived from **2**, 1-Ph_2P=N($SiMe_3$)-C_6H_4-2-(Ph_2P)Rh(CO)Cl, **15** was structurally characterized. Crystal data for **15**: crystal dimensions, 0.32 × 0.44 × 0.66 mm; space group, monoclinic, $P2_1/c$ (No. 14); a = 13.793(3) Å, b = 12.622(11) Å, c = 20.436(6) Å, β = 105.93(2)°, V = 3421.2 Å^3, Z = 4. Final R, R_w, and GOF values were 0.064, 0.061, and 1.45 respectively. The complex shows typical square planar geometry about Rh, a *cis* phosphine−CO relationship, and no exceptional steric crowding of the coordination site.

Introduction

We have previously described a number of phosphoranimino−phosphine ligands obtained by Staudinger[1] oxidation of bis(phosphines) and the metal complexes derived from these versatile ligands.[2−11] It was of interest to explore the related chemistry of 1,2-bis(diphenylphosphino)benzene (**1**) because of the effects which could arise in such a case from constraining the two phosphine substituents to a *cis* orientation on the phenyl backbone. Beneficial effects which might be introduced by the aromatic character of the backbone could also be of interest. The rigid phenyl backbone also provides a reference plane for the angular phosphine−imine backbone allowing the detection of isomers should they exist. The results of this study indicated that the system provided unusual steric control of the oxidation with azides such that only one phosphorus is oxidized in contrast to the more usual oxidation of both phosphines with sulfur, selenium, and oxo agents. The asymmetrically substituted (iminophosphorano)phosphine ligands are also good chelating agents utilizing the phosphine and imine nitrogen centers.

Results and Discussion.

Synthesis of 1,2-Bis(diphenylphosphino)benzene (1). There are a variety of synthetic methods described in the literature[12−16] for the production of 1,2-bis(diphenylphosphino)benzene (**1**) and related species. Tunney and Stille[16] describe the coupling of diphenyl(trimethylsilyl)phosphine with 2-bromoiodobenzene in the presence of a palladium catalyst to produce (2-bromophenyl)diphenylphosphine. Subsequent lithiation and reaction with chlorodiphenylphosphine produces **1**. The higher yield (Tunney and Stille[16] report an overall yield of 75%—ours was a bit lower), the milder reagents, and the ease of synthesis of the starting materials make this route is the method of choice (eq 1).

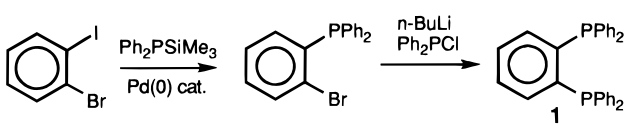

(1)

Reaction of 1 with Azides. Limited Azide Oxidation of Hindered Bis(phosphines). Reactions of **1** with azides are

[⊗] Abstract published in *Advance ACS Abstracts,* June 1, 1996.

(1) Staudinger, H.; Meyer, J. *Helv. Chim. Acta* **1919**, *2*, 635.
(2) Balakrishna, M. S.; Santarsiero, B. D.; Cavell, R. G. *Inorg. Chem.* **1994**, *33*, 3079.
(3) Balakrishna, M.; Klein, R.; Uhlenbrock, S.; Pinkerton, A. A.; Cavell, R. G. *Inorg. Chem.* **1993**, *32*, 5676.
(4) Cavell, R. G.; Reed, R. W.; Katti, K. V.; Balakrishna, M.; Collins, P. W.; Mozol, V.; Bartz, I. *Phosphorus, Sulfur Silicon* **1993**, *76*, 9.
(5) Katti, K. V.; Santarsiero, B. D.; Pinkerton, A. A.; Cavell, R. G. *Inorg. Chem.* **1993**, *32*, 5919.
(6) Katti, K. V.; Cavell, R. G. *Comments Inorg. Chem.* **1990**, *10*, 53.
(7) Katti, K. V.; Batchelor, R. J.; Einstein, F. W. B.; Cavell, R. G. *Inorg. Chem.* **1990**, *29*, 808.
(8) Katti, K. V.; Cavell, R. G. *Organometallics* **1989**, *8*, 2147.
(9) Katti, K. V.; Cavell, R. G. *Inorg. Chem.* **1989**, *28*, 3033.
(10) Katti, K. V.; Cavell, R. G. *Inorg. Chem.* **1989**, *28*, 413.
(11) Katti, K. V.; Cavell, R. G. *Organometallics* **1988**, *7*, 2236.
(12) McFarlane, H. C. E.; McFarlane, W. *Polyhedron* **1983**, *2*, 303.
(13) Talay, R.; Rehder, D. *Z. Naturforsch., B* **1981**, *36B*, 451.
(14) Kyba, E. P.; Kerby, M. C.; Rines, S. P. *Organometallics* **1986**, *5*, 1189.
(15) Kyba, E. P.; Liu, S. T.; Harris, R. L. *Organometallics* **1983**, *2*, 1877.
(16) Tunney, S. E.; Stille, J. K. *J. Org. Chem.* **1987**, *52*, 748.

S0020-1669(95)01471-6 CCC: $12.00

Scheme 1

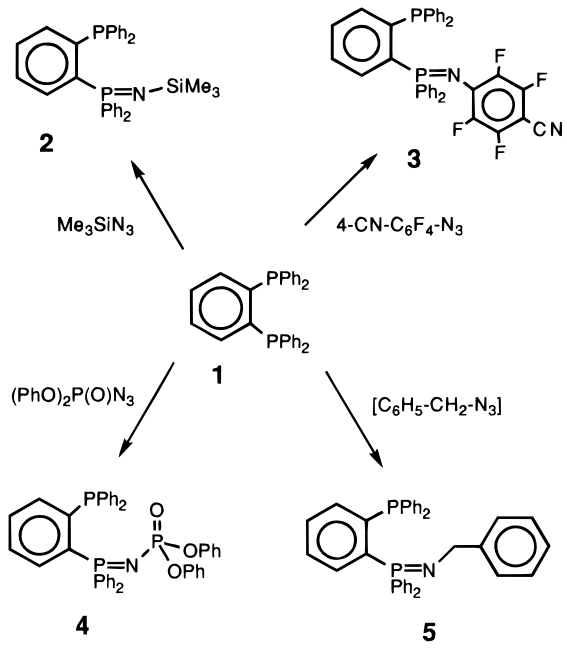

summarized in Scheme 1. Although we earlier[10] found that the preferred synthetic strategy for the reaction of alkanediylbis(phosphines) with trimethylsilyl azide involved conducting the reaction in the absence of solvent at temperatures exceeding the melting point of the bis(phosphine) utilizing a very efficient reflux condenser, here the melting temperature of (**1**) (179−181 °C) is 100 °C higher than the boiling point of trimethylsilyl azide (95−97 °C)[17]) and the azide undergoes pyrolysis before the reagents can form a homogeneous melt. For the trimethylsilylazide conversion of **1** to **2** we therefore used a high boiling solvent such as toluene as the reaction medium. It was also necessary to monitor the reaction to ensure that complete reaction was achieved while at the same time avoiding reaction of the azide with the solvent. This was accomplished by careful monitoring of the progress of reaction by ^{31}P NMR spectroscopy and the periodic addition of additional azide throughout.

Reaction of **1** with several other azides proceeded in a similarly straightforward fashion with reactions occurring at or below room temperature, again in a solvent. *p*-cyanotetrafluorophenyl azide reacts with **1** at −78 °C induced an immediate color change in the reaction solution which suggests that the reaction occurs at low temperature; however, slow warming to room temperature with an overnight reaction time was our standard procedure so the actual temperature at which the reaction began is uncertain. The reactions of diphenoxyphosphoryl azide and benzyl azide with **1** also proceeded smoothly with the same result; the formation of only the monooxidized (iminophosphorano)phosphine. The products of these reactions have very different physical characteristics. **3** is a highly crystalline solid with limited solubility in polar solvents and is insoluble in nonpolar solvents but it is however readily recrystallized from acetonitrile. The trimethylsilanimine (**2**), phenylmethanimine (**5**), and oxodiphenoxyphosphoranimine (**4**) derivatives are highly soluble materials. The former pair, **2** and **5**, can be easily purified by hexane extraction followed by recrystallization from acetonitrile. The oxodiphenoxyphosphorane derivative, **4**, however produced viscous oils from most recrystallizing solvents. We found the best method for the isolation of pure samples of this imine was simply to use precise stoichiometry with careful control of reaction conditions and, upon completion of the reaction, to remove the solvent *in vacuo*. This method produced an amorphous powder of **4** of sufficient purity for subsequent chemistry.

Table 1. ^{31}P NMR Data for the Precursors and Derivatives

compound	$\delta(^{31}P^{III})$ (ppm)	$\delta(^{31}P^{V})$ (ppm)	$^3J_{PP}$ (Hz)
1	−13.6		
2	−14.8	1.2	17.8
3[a]	−15.9	13.8	21.0
4[b]	−15.9	13.8	23.6
5	−13.9	10.3	15.0
6[c]	−16.3	27.0	26.0
7[c]	−13.8	30.1	14.9
8[c]		34.1	
9[c]		47.5	
10	−23.06		
11	−7.47		
12	−23.7[d]	2.06	12.5
13	−4.42[e]	7.84	15.3
14		21.73	

[a] $^4J_{PF}$ = 4.5 Hz. [b] Phosphinic phosphorus δ = −8.9 ppm, $^2J_{PP}$ = 36.2 Hz. [c] Not isolated. [d] $^4J_{PF}$ = 5.5 Hz, $^7J_{PF}$ = 6.7 Hz. [e] $^4J_{PF}$ = 5.2 Hz.

Selective Oxidation. Unlike the bis(phosphines) with flexible alkane backbones (e.g. dppm),[10] **1** was never doubly oxidized with trimethylsilyl azide. Even prolonged reflux of concentrated toluene solutions of **1** with an excess of azide failed to show any evidence of oxidation of the second phosphine center; only **2** was obtained in almost quantitative yield. The other azide reactions behaved similarly, producing only the oxidation of only one of the two phosphine centers. In contrast to these azide oxidations, both phosphorus atoms in **1** are readily oxidized by S, Se, or H_2O_2. We postulate that the failure to induce reaction at the second phosphine center is a direct result of steric crowding created by the rigid *cis* configuration of the phosphorus centers which inhibits the reaction mechanism. In contrast, chalcogen oxidizers, proceeding by means of a different mechanism, readily oxidize both phosphine centers in the *o*-bis(diphenylphosphino)benzene. The mechanism of the Staudinger reaction between a phosphine and an azide has been extensively investigated,[18−20] and it is accepted that the reaction proceeds *via* attack of the terminal nitrogen on the phosphine and the formation of a cyclic intermediate incorporating that phosphine center. The subsequent elimination of N_2 from this intermediate yields the imine. The need to form the cyclic intermediate means that steric crowding can inhibit the reaction and a second oxidation at an adjacent site is more susceptible to such a constraint than the first.

There is also the possibility in these systems that an "electronic cooperativity" exists between the two phosphorus centers which is transmitted through the aromatic backbone. This hypothesis was tested by comparing the azide oxidation processes for the unsaturated bis(phosphines), *cis*-1,2-bis(diphenylphosphino)ethylene, **10**, and *trans*-1,2-bis(diphenylphosphino)ethylene, **11**,[21] using 4-cyanotetrafluorophenyl azide[22] which is easily made and which is relatively reactive, more so than Me_3SiN_3. The reactions were conducted under identical conditions and monitored by removing small portions of each reaction mixture periodically for analysis by ^{1}H and ^{31}P NMR spectroscopy. The NMR spectra revealed that **10**

(17) Washburne, S. W.; Peterson, W. R., Jr. *J. Organomet. Chem.* **1971**, *33*, 153.
(18) Gololobov, Y. G.; Kasukhin, L. F. *Tetrahedron* **1992**, *48*, 1353.
(19) Gololobov, Y. G.; Zhmurova, I. N.; Kasukhin, L. F. *Tetrahedron* **1981**, *37*, 437.
(20) Gololobov, Y. G.; Kasukhin, L. F. *Russ. J. Gen. Chem. (Engl. Transl.)* **1979**, *49*, 831.
(21) Aguiar, A. M.; Daigle, D. *J. Am. Chem. Soc.* **1964**, *86*, 2299.
(22) Keana, J. F. W.; Cai, S. X. *J. Fluorine Chem.* **1989**, *43*, 151.

reacts smoothly with the azide to produce only **12**, the singly oxidized imine. Under the same conditions, **11** produces both **13** and the doubly oxidized product, **14**, at similar rates. Thus the selectivity of oxidation of **1** is most likely controlled by the steric crowding of the phosphorus centers imposed by the rigid benzene (or ethylene) backbone and the proximity of the *ortho* substituents. The steric interferences are lifted in the *trans*-bis(phosphino)ethylene (**11**), and oxidation of both phosphine centers proceeds apace in spite of the fact that the two phosphine centers are connected by an unsaturated bridge.

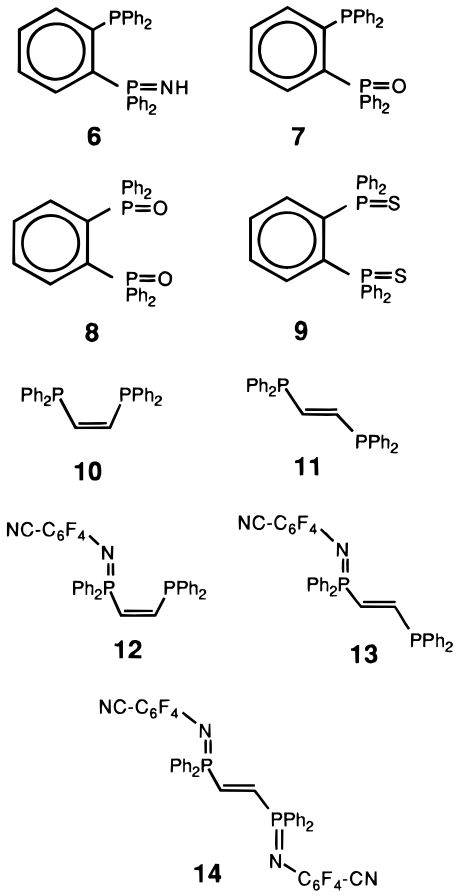

Spectroscopy. Multinuclear NMR spectroscopy gives clear characterization of the all iminophosphorane−phosphine products as the asymmetry of the reaction products yields well defined ^{31}P NMR AX spin systems.[23] Table 1 contains a summary of the ^{31}P NMR data for the various 1-(diphenylphosphinimino)-2-(diphenylphosphino)benzene derivatives. The starting material, **1**, displays a single resonance in the ^{31}P NMR spectrum at −13.6 ppm (lit. -14.2 ppm[16]). Oxidation of one phosphine center produces a large chemical shift change with creation of the P^V center (which is deshielded by 20−60 ppm depending om the imine substituent) but leaves the chemical shift of the P^{III} center relatively unaffected. This is in contrast to the behavior of dppm and the amine-bis(phosphine) analogs wherein both the P^{III} and the P^V signals shift markedly on imine formation at one center.[2−11]

For the *N*-trimethylsilyl derivative **2**, ^{31}P NMR spectroscopy identifies the AX spin system [P^{III}, −14.8 ppm; P^V, 1.2 ppm; $^3J_{PP}$ = 17.8 Hz]. Proton NMR spectroscopy shows one trimethylsilyl group with a single line resonance at 0.04 ppm. The ^{13}C and ^{29}Si NMR spectra of the trimethylsilyl group show coupling to the phosphorus through the P═N−Si linkage. The ^{13}C chemical shift is 5.6 ppm, the ^{29}Si shift is −12.1 ppm, and the coupling constants are $^3J_{CP}$ = 3.0 Hz and $^2J_{SiP}$ = 20.8 Hz.

Reactions of **2** were carried out in order to establish the ^{31}P NMR chemical shifts of hydrolysis and oxidation products and to ascertain whether the monochalcogen derivatives of **1** were accessible *via* this route. The addition of five drops of methanol to a NMR sample of **2** immediately produced a new AX spectrum which we assign to the free phosphinimine derivative **6** (P^{III}, −16.3 ppm; P^V, 27.0 ppm; $^3J_{PP}$ = 26.0 Hz). Such imines cannot normally be isolated.[24] The reaction of **2** with a small amount of water in toluene solution for 5 days produced the ^{31}P NMR spectrum tentatively assigned to **7**, the monooxide of **1** (P^{III}, −13.8 ppm; P^V, 30.1 ppm; $^3J_{PP}$ = 14.9 Hz). In addition, the "ylidic" phosphinimine linkage undergoes Wittig-like reactions with benzaldehyde to produce **7** and *N*-(trimethylsilyl)-phenylmethanimine. Further reactions of **1** with excess H_2O_2 or sulfur produced the corresponding doubly oxidized derivatives, **8** and **9,** which showed singlets with ^{31}P NMR chemical shifts of 34.1 ppm and 47.5 ppm respectively.

The *p*-cyanotetrafluorophenyl monoimine **3** is clearly identified by ^{31}P NMR spectroscopy (P^{III}, −15.9 ppm; P^V, 13.8 ppm; $^3J_{PP}$ = 21.0 Hz). In addition, a small phosphorus−fluorine coupling is observed in the P(V) resonance, $^4J_{PF}$ = 4.5 Hz. A curious feature of **3** is that a $^7J_{P(V)F}$ coupling of 6.7 Hz was observed. In the absence of structural evidence it can only be speculated that there is a close phosphorus(III)−fluorine contact responsible for this unusual coupling. The absence of a similar coupling in **12**-**14** suggests that the coupling arises *via* a "through space" interaction and not through a "seven-bond" interaction.

The diphenoxyphosphoryl azide gave **4**, a compound with three distinct phosphorus centers showing an expected AMX[23] ^{31}P NMR spectrum (P^{III}, −15.9 ppm; $P_N{}^V$, 13.8 ppm; $P_O{}^V$, −8.9 ppm; $^2J_{PP}$ = 36.2 Hz, $^3J_{PP}$ = 23.6 ppm).

The benzyl azide (prepared *in situ*) from benzyl bromide on an Amberlite ion exchange resin that had been treated with sodium azide[25] gave **5** (P^{III}, −13.9 ppm; P^V, 10.3 ppm; $^3J_{PP}$ = 15.0 Hz). Herein ^{1}H NMR clearly identifies the benzyl protons (4.5 ppm; $^3J_{PH}$ = 17 Hz).

The P^{III} chemical shifts of **12** and **13**, wherein the phosphorus atoms are connected by an ethylene backbone, change only slightly from the values in **10** and **11** (−23.04 and −7.47 ppm) compared to the much larger chemical shift changes experienced by the remote P(V) center. The $^3J_{PP}$ coupling constants in **12** and **13** are of similar magnitude, with the *trans* coupling in **13** being slightly larger (by approximately 3 Hz) than the *cis*.[23]

X-ray Crystallography of 2. An X-ray structural analysis of **2** was prompted by the unique resistance of this compound to double oxidation by azides. The experimental details are tabulated in Tables 2−5 and the molecular structure is illustrated in Figure 1. The rigid backbone, P(1)−C(1)−C(2)−P(2), is essentially planar (maximum displacement from plane 0.04Å), and the phosphorus−nitrogen double bond forms a dihedral angle of 60° from this plane. The lone pair of electrons on the phosphorus(III) and on the imine nitrogen atom extend in an overlapping fashion into the open mouth of the ligand and suggest a promising chelating ability. Furthermore, the bulk of the $SiMe_3$ group and the disposition of the electron pairs on phosphorus and nitrogen indicate reasons for the resistance of **2** to undergo further oxidation with a second mole of azide; the phosphine center is somewhat crowded, and the space required to form the cyclic triazide intermediate necessary for progression

(23) Becker, E. D., *High Resolution NMR*, 2nd ed.; Academic Press Inc.: New York, 1980.

(24) Johnson, A. W. *Ylides and Imides of Phosphorus;* Wiley: New York, 1993.

(25) Hassner, A.; Stern, M. *Angew. Chem., Int. Ed. Engl.* **1986**, *25*, 478.

Table 2. Crystallographic Experimental Details for **2** and **15**

	2	**15**
	A. Crystal Data	
formula	$C_{33}H_{33}NP_2Si$	$C_{34}H_{33}ClNOP_2RhSi$
fw	533.67	700.03
cryst dimens (mm)	0.38 × 0.38 × 0.57 mm	0.32 × 0.44 × 0.66 mm
space group	monoclinic, $P2_1/c$ (No. 14)[a]	monoclinic, $P2_1/c$ (No 14)[a]
a (Å)	11.093(5)	13.793(3)
b (Å)	14.898 (5)	12.622(11)
c (Å)	18.811(2)	20.436(6)
β (deg)	102.76(2)	105.93(2)
V (Å$^{3)}$	3031	3421.2
Z	4	4
D_c (g cm^{-1})	1.169	1.359
μ (cm^{-1})	1.99	7.214
	B. Data Collection and Refinement Conditions	
radiation	Mo Kα (λ = 0.710 73 Å)	Mo Kα (λ = 0.710 73 Å)
diffractometer	Enraf-Nonius CAD-4	Enraf-Nonius CAD-4
monochromator	incident beam, graphite crystal	incident beam, graphite crystal
temp (°C)	23	−20
take-off angle (deg)	3.00	3.00
detector aperture (mm)	2.40 horiz × 4.0 vert	2.40 horiz × 4.0 vert
crystal-to-detector dist (mm)	205	205
scan type	$\theta-2\theta$	$\theta-2\theta$
scan rate (deg min^{-1})	1.0−2.5	2.0−4.0
scan width	0.800 + 3.34 tan θ	0.900 + 0.347 tan θ
data collcn 2θ limit (deg)	56	56
data collcn index range	$-h, -k, \pm l$	$-h, -k, \pm l$
no of reflcs	7542 total	8589 total
no. averaged with $I > 2.50\sigma_I$	2941	3537
observns/variables ratio	2941/334	3537/370
structure solution method	direct methods[b]	three dimensional Patterson[c]
refinement method	full matrix on F[d]	full matrix on F[d]
cor applied	empirical abs cor[e]	empirical abs cor[e]
agreement factors		
R_1[f]	0.068	0.064
R_2[g]	0.074	0.061
GOF	1.92	1.45

[a] *International Tables for X-Ray Crystallography*, The Kynoch Press: Birmingham, England, 1969; Vol I. [b] Gilmore, C. J. MITHRIL 83, A Multiple Solution Direct Methods Program. University of Glasgow. [c] The Rh and P atom positions were derived from a three dimensional Patterson map and the remaining non-hydrogen atoms were located from a set of difference Fourier maps. [d] The computer programs used in this analysis include the Enraf-Nonius Structure Determination Package, Version 3 (1985, Delft, The Netherlands), adapted for a SUN Microsystems 3/160 computer and several locally written programs by Dr. R. G. Ball. [e] Walker, N.; Stuart, D., Acta Crystallog., **1983**, *A39*, 158. [f] $R_1 = \sum||F_o| - |F_c||/\sum|F_o|$. [g] $R_2 = (\sum w(|F_o| - |F_c|)^2/\sum wF_o^2)^{1/2}$.

to the imine product is limited. The rigid phenyl backbone prevents the relief of this steric congestion through bond rotation and thus the formation of a second phosphazide intermediate is strongly inhibited even under strenuous reaction conditions.

The P═N and N−Si bond lengths (1.529(5) and 1.672(5) Å), are similar to those found for $Me_3P{=}N{-}SiMe_3$ (1.542(5) and 1.705(5) Å)[26] and $Ph_2PCH_2P(Ph_2){=}N{-}SiMe_3$ (1.529(3) and 1.668(3) Å).[27] The P═N−Si bond angles for the silylated imines are large, *c.f.* 152.7(3)° for **2**, 150.2(2)° [27] for $Ph_2PCH_2P(Ph_2){=}N{-}SiMe_3$ and 144.6(1.1)° [26] for $Me_3P{=}N{-}SiMe_3$. Indeed the P═N−Si angle in these molecules is more closely reminiscent of the near linear (N-trimethylsilyl−imido)metal systems (*e.g.*, $Cl_3V{-}N{-}SiMe_3$, ∠V═N−Si = 177.5(1)°)[28] rather than the P═N−C systems in which the nitrogen atom adopts the more classical sp^2-hybridized geometry (*e.g.*, $Ph_2FP{=}NMe$, ∠P═N−C =119°)[29] and in related molecules prepared by us, $Ph_2PCH_2PPh_2{=}NAr$ [Ar = 5-F,2,4-$(NO_2)_2C_6H_2$, (wherein P═N is 1.589(5) Å and the P−N−Ar angle is 128.8-(4)°) and Ar = 4-(CN)C_6F_4 (wherein the P═N distance is 1.567-(4) Å and the P−N−Ar angle is 132.9(3)°)].[5]

Theoretical calculations[30−33] for phosphazene systems and our own *ab initio* studies[34] on the models $H_3P{=}N{-}SiH_3$ and $H_3P{-}N{-}PH_3^+$, reveal pairs of orthogonal, high-lying occupied molecular orbitals localized on nitrogen with significant d-orbital contributions from phosphorus and silicon.[34] One of these orbitals represents the phosphorus−nitrogen double bond, and the other orbital represents the diffusion of the nitrogen lone pair of electrons into the more electropositive phosphorus and silicon centers. This produces strong, yet hydrolytically unstable, bonding in the P═N−Si linkage. This view of the bonding in the P═N−Si unit is in agreement with the photoelectron spectroscopic studies of $Ph_3P{=}N{-}SiMe_3$ and $Me_3P{=}N{-}SiMe_3$.[33] These two compounds display only one low ionization potential in the photoelectron spectrum corresponding to the two highest occupied molecular orbitals. In contrast, similar compounds with P═N−C or P═N−H linkages

(26) Astrup, E. E.; Bouzga, A. M.; Starzweski, K. A. O. *J. Mol. Struct.* **1987**, *51*, 51.
(27) Schmidbaur, H.; Bowmaker, G. A.; Kumberger, O.; Müller, G.; Wolfsberger, W. *Z. Naturforsch., B* **1990**, *45B*, 476.
(28) Schweda, E.; Scherfise, K. D.; Dehnicke, K. *Z. Anorg. Allg. Chem.* **1985**, *528*, 117.
(29) Adamson, G. W.; Bart, J. C. J. *J. Chem. Soc., Chem. Commun.* **1969**, 1036.
(30) Wheeler, R. A.; Hoffmann, R.; Strähle, J. *J. Am. Chem. Soc.* **1986**, *108*, 5381.
(31) Schmidt, M. W.; Gordon, M. S. *Inorg. Chem.* **1986**, *25*, 248.
(32) Schoeller, W. W.; Busch, T.; Niecke, E. *Chem. Ber.* **1990**, *123*, 1653.
(33) Starzewski, K. A. O.; Dieck., H. T. *Inorg. Chem.* **1979**, *18*, 3307.
(34) Calculations were carried out using MONSTERGAUSS (closed shell, SCF, ab-initio calculations) The basis set was STO-3G* (d-orbitals for phosphorus) with full geometry optimization for non-hydrogen atoms.

Table 3. Atomic Coordinates ($\times 10^4$) and Equivalent Isotropic Gaussian Parameters (Å $\times$ 10^3) for **2**

atom	*x*	*y*	*z*	*U*(eq)[a]
P(1)	2116(1)	1121(1)	4172.5(8)	45.0(4)
P(2)	818(1)	1090(1)	2448.3(8)	43.7(4)
Si	3990(2)	2379(1)	3655(1)	70.5(7)
N	3079(4)	1538(3)	3803(2)	53(2)
C(1)	1533(4)	68(3)	3729(3)	42(2)
C(2)	956(4)	48(3)	2993(3)	42(2)
C(3)	525(5)	−767(3)	2679(3)	58(2)
C(4)	649(6)	−1552(4)	3077(3)	72(3)
C(5)	1216(6)	−1525(4)	3804(4)	77(3)
C(6)	1656(5)	−724(4)	4130(3)	62(2)
C(7)	5003(7)	2780(6)	4499(4)	174(4)
C(8)	4976(5)	2015(5)	3037(3)	90(3)
C(9)	3044(7)	3343(5)	3188(5)	141(4)
C(11)	2715(5)	863(4)	5125(3)	54(2)
C(12)	3961(6)	704(5)	5359(4)	84(3)
C(13)	4472(7)	484(6)	6087(4)	124(4)
C(14)	3728(6)	444(5)	6582(4)	94(3)
C(15)	2504(6)	609(4)	6360(3)	72(3)
C(16)	1979(5)	818(4)	5646(3)	60(2)
C(21)	726(4)	1763(3)	4174(3)	44(2)
C(22)	−421(5)	1367(4)	4089(3)	61(2)
C(23)	−1460(5)	1874(5)	4113(3)	73(3)
C(24)	−1358(6)	2783(4)	4220(4)	81(3)
C(25)	−216(6)	3184(4)	4318(4)	92(3)
C(26)	826(5)	2670(4)	4301(3)	68(2)
C(31)	1986(4)	924(4)	1910(3)	48(2)
C(32)	2153(5)	1643(4)	1467(3)	67(2)
C(33)	2999(5)	1599(5)	1043(3)	90(3)
C(34)	3708(5)	830(5)	1059(3)	90(3)
C(35)	3586(6)	131(5)	1514(3)	86(3)
C(36)	2713(5)	180(4)	1937(3)	68(2)
C(41)	−600(5)	867(3)	1778(3)	46(2)
C(42)	−673(5)	560(4)	1080(3)	62(2)
C(43)	−1797(5)	433(4)	595(3)	75(3)
C(44)	−2864(5)	632(5)	826(4)	85(3)
C(45)	−2821(6)	943(5)	1515(4)	89(3)
C(46)	−1692(5)	1049(4)	1985(3)	66(2)

[a] The equivalent isotropic Gaussian parameter *U*(eq) is $^1/_3\sum r_i^2$ (i = 1−3), where r_i's are the root-mean-square amplitudes of the AGDP's (anisotropic Gaussian displacement parameters for **2**).

Table 4. Selected Interatomic Bond Lengths (Å) for **2**[a]

N−P(1)	1.529(5)	P(1)−C(1)	1.827(5)
Si−N	1.672(5)	P(2)−C(2)	1.847(5)
Si−C(7)	1.831(8)	P(1)−C(11)	1.809(5)
Si−C(8)	1.845(7)	P(1)−C(21)	1.814(5)
Si−C(9)	1.879(7)	P(2)−C(31)	1.829(6)
		P(2)−C(41)	1.816(5)

[a] Phenyl carbon−carbon bond lengths are omitted. The backbone phenyl ring shows bond lengths of 1.382(9) Å with no systematic variations around the ring.

Table 5. Selected Interatomic Angles (deg) for **2**

Si−N−P(1)	152.7(3)	C(1)−P(1)−C(11)	106.5(2)
N−P(1)−C(1)	110.7(3)	C(1)−P(1)−C(21)	103.8(2)
N−P(1)−C(11)	113.3(2)	C(2)−P(2)−C(31)	102.2(2)
N−P(1)−C(21)	117.8(2)	C(2)−P(2)−C(41)	100.7(2)
N−Si−C(7)	112.2(3)	C(7)−Si−C(8)	107.9(3)
N−Si−C(8)	110.4(3)	C(7)−Si−C(9)	109.2(4)
N−Si−C(9)	110.8(3)	C(8)−Si−C(9)	106.1(4)
P(1)−C(1)−C(2)	120.8(4)	P(2)−C(2)−C(1)	119.8(4)
P(1)−C(1)−C(6)	119.9(4)	P(2)−C(2)−C(3)	121.3(4)
P(1)−C(11)−C(12)	118.5(5)	P(2)−C(31)−C(32)	115.6(4)
P(1)−C(11)−C(16)	123.8(4)	P(2)−C(31)−C(36)	125.0(5)
P(1)−C(21)−C(22)	122.4(4)	P(2)−C(41)−C(42)	125.7(4)
P(1)−C(21)−C(26)	118.9(4)	P(2)−C(41)−C(46)	116.6(4)
C(11)−P(1)−C(21)	103.7(3)	C(31)−P(2)−C(41)	101.6(2)

show two ionization potentials, one which can be attributed to the nitrogen lone pair of electrons and one which can be assigned to a P═N π bond.

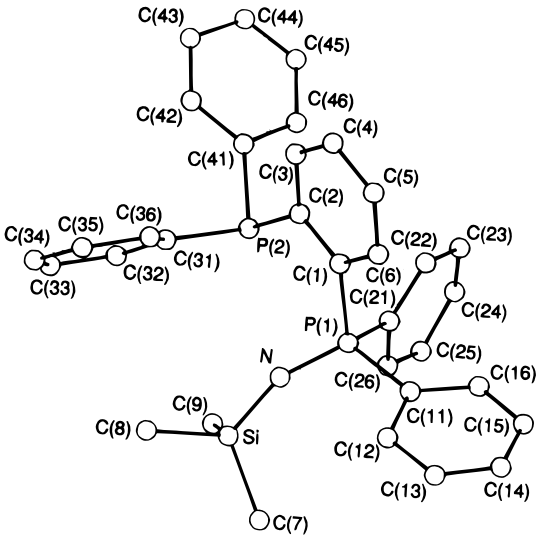

Figure 1. Representation of the molecular structure of **2** showing the atom numbering scheme. Atoms are shown as Gaussian ellipsoids at the 20% probability level.

Table 6. Selected ^{31}P NMR and IR Data[a] for the Rhodium Complexes

complex	δ(P(III)) (ppm)	$^1J_{PRh}$ (Hz)	$^3J_{PP}$ (Hz)	δ(P^V)[b] (ppm)	ν_{CO} (cm^{-1})
15	40.45 dd	175.2	19.1	20.2 dd[b]	1980
16	36.52 dd	169.6	27.9	27.8 d	1986
17[c]	50.0 dd	170.6	20.1	40.5 "t"	1986
18	29.73	171.0	34.7	15.24	1989

[a] dd = doublet of doublets, d = doublet, "t" = triplet (overlapping doublet of doublets). [b] $^2J_{PRh}$ = 1.9 Hz. [c] P(O)(OPh)$_2$ δ 7.3 ppm, $^2J_{PP}$ = 18.5 Hz.

Complexes with [Rh(CO)$_2$Cl]$_2$. Representative rhodium complexes were prepared by reaction of **2**, **3**, and **4** with [Rh(CO)$_2$Cl]$_2$ to form the corresponding complexes **15**, **16**, and **17.** With **12**, **18**, was obtained. The ^{31}P NMR and selected infrared spectroscopy data for these compounds are listed in Table 6.

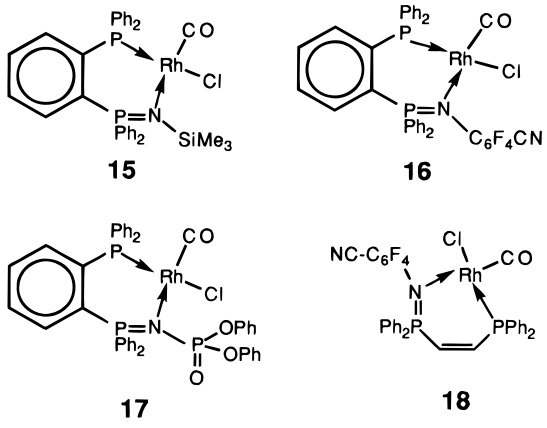

The ^{31}P NMR spectrum of **15** reveals a large coordination shift effect on the P^{III} (the coordination shift is +55 ppm) similar to those observed in related systems.[2,3] The large $^1J_{PRh}$ coupling constant associated with that signal (175.2 Hz) clearly identifies the coordinated P^{III} resonance. Likewise, the smaller change in the P^V (coordination shift +19 ppm) and the presence of a small $^2J_{PRh}$ coupling constant (1.9 Hz) demonstrates chelate formation. Proton (−0.29 ppm), ^{13}C (5.6 ppm; $^3J_{CP}$ = 5.6 Hz), and ^{29}Si (6.6 ppm; $^2J_{SiP}$ = 5 Hz) NMR spectroscopy all demonstrate that the P═N−Si linkage remains intact. Infrared spectroscopy recorded an intense absorption at 1980 cm^{-1}

attributed to a single carbonyl on the rhodium center, and in the mass spectrum an intense signal was detected at mass number 671 (87.5%), assigned to loss of carbon monoxide from the parent ion.

In a similar fashion, the complex **16** displays the same characteristic NMR signals. The P(III) chemical shift and coupling constants (36.5 ppm; $^1J_{PRh} = 169.6$ Hz, $^3J_{PP} = 27.9$ Hz) are very similar; however, the broad P^V signal is not as well resolved (27.8 ppm) masking additional structural information from long-range fluorine and rhodium coupling constants. The poor solubility of this complex resulted in limited detection of aromatic ^{13}C NMR signals, and ^{19}F NMR spectroscopy revealed two poorly resolved complex multiplets. Infrared spectroscopy detected the strong carbonyl absorption at 1986 cm^{-1} for **16**, similar to **15** (1980 cm^{-1}), suggesting similar stereochemistry for the rhodium center.

The oxodiphenoxyphosphoranimine derivative **17** also displays characteristic spectroscopic features similar to **15** and **16** but the incorporation of an additional phosphorus center produces a more complicated ^{31}P NMR spectrum. The deshielded P^{III} resonance is clearly identified by the large rhodium coupling constant (50 ppm; $^1J_{PRh} = 170.6$ Hz, $^3J_{PP} = 20.1$ Hz). The imine $P_N{}^V$ center (40.5 ppm) appears as an overlapping doublet of doublets due to coupling constants of similar magnitude to the terminal phosphinic group (7.3 ppm; $^2J_{PP} = 18.5$ Hz) and the phosphine. The greater solubility of this complex enabled the detection of the rhodium carbonyl signal (IR: ν(CO) = 1986 cm^{-1}) in the ^{13}C NMR spectrum (185.9 ppm; $^1J_{CRh} = 78.5$ Hz, $^2J_{CP} = 16.2$ Hz). The coupling constants are in the expected range for a carbonyl *cis* to the P^{III} center on rhodium, and a similar infrared stretching frequency for the carbonyl suggests the same stereochemistry prevails for all three complexes.

The complex **18** shows ^{13}C NMR data for the carbonyl ligand ($\delta = 186.8$ ppm; $^1J_{CRh} = 72.5$ Hz, $^2J_{CP} = 19.6$ Hz) and an IR stretching frequency for the carbonyl ligand (1996 cm^{-1}) suggesting a stereochemistry similar to that of **15**−**17**. Thus **18** is square planar about rhodium with the carbonyl ligand *cis* to the P^{III} center of the chelating ligand. The ^{31}P NMR data (P^{III} 29.73 ppm; $^1J_{PRh} = 171.0$ Hz, $^3J_{PP} = 37.4$ Hz; P^V 15.24 ppm; $^3J_{PP} = 37.6$ Hz) also demonstrate chemical shift complexation changes similar to those obtained for the complexes derived from the ligand with an aromatic backbone. In contrast to **16**, however, the $^3J_{PP}$ coupling constant increases significantly from 12.5 to 37.5 Hz upon complexation to rhodium. Since the vicinal proton resonances are masked by the aromatic resonances in the ^1H NMR spectrum, there is little evidence to indicate the source of this larger coupling constant. The IR spectra of **12** and **14** suggest however that the ethylene carbon−carbon double bond is apparently unaffected by the imine formation on the phosphine centers as indicated by stretching frequencies of 1644 and 1643 cm^{-1} respectively.

X-ray Crystallography of 15. An X-ray structural analysis of **15** revealed the stereochemistry of the rhodium center and the effect of coordination upon the P═N−Si linkage. The experimental details are given in Tables 2 and 7−9 and the molecular structure is illustrated in Figure 2. The rhodium center is square planar with the carbonyl ligand *cis* to the P(III) center as anticipated from ^{13}C NMR spectroscopy on the oxodiphenoxyphosphoranimine derivative.

The overall structure of the ligand is unchanged with the exception of the P═N−Si unit. The P(1)−C(1)−C(2)−P(2) backbone is planar (maximum deviation 0.15Å). The P═N−Si linkage forms a plane with a dihedral angle of 58.8° above the P(1)−C(1)−C(2)−P(2) plane, and the plane defined by the four atoms joined to the rhodium center defines a dihedral angle of 43.5° below the P(1)−C(1)−C(2)−P(2) plane. The six-membered heteroatom ring formed from these planar units is highly distorted (see Figure 2).

The structure of the chelate is similar to that of complexes of related ligands wherein the phosphorus centers are connected by CH_2[5] or NR bridges.[2] Most notably there is a similar lengthening of the P═N bond upon coordination[2,5] to 2.215(10) Å in the case of the phosphonocimine−Rh complex and 2.141(2) Å in the case of the fluoroaromatic−Rh complex. There are however also additional ring size features in these latter cases which form five-membered rings which may play a role in the determination of the parameters. The present system involves a six-membered chelate ring.

Table 7. Atomic Coordinates ($\times 10^4$) and Equivalent Isotropic Gaussian Parameters (Å $\times 10^3$) for **15**

atom	*x*	*y*	*z*	*U*(eq)[a]
Cl	1620(2)	2529(2)	−780(1)	69.3(10)
N	2418(4)	3149(6)	839(3)	41(2)
P(1)	1845(2)	2738(2)	1363(1)	40.2(8)
P(2)	3815(2)	1260(2)	1186(1)	38.0(7)
Rh	2729.3(5)	1844.7(6)	253.2(3)	38.7(2)
Si	2820(2)	4390(2)	684(1)	60(1)
C	2971(6)	662(8)	−270(4)	63(4)
O	3086(5)	18(6)	−579(3)	39(3)
C(1)	2588(5)	1907(7)	2037(3)	40(3)
C(2)	3414(5)	1307(7)	1971(3)	35(3)
C(3)	3918(6)	661(7)	2508(4)	47(3)
C(4)	3616(6)	598(7)	3096(4)	54(3)
C(5)	2812(6)	1149(8)	3159(4)	53(3)
C(6)	2294(6)	1815(8)	2645(3)	50(3)
C(7)	3730(7)	4282(9)	165(5)	90(5)
C(8)	1741(8)	5188(9)	204(6)	124(6
C(9)	3502(8)	5069(9)	1488(5)	113(6)
C(11)	769(6)	1964(8)	945(4)	47(3)
C(12)	485(7)	1044(9)	1236(4)	77(4)
C(13)	−337(8)	458(12)	893(5)	134(6)
C(14)	−859(9)	768(12)	268(5)	149(6)
C(15)	−618(7)	1669(11)	−35(5)	113(6)
C(16)	205(6)	2249(9)	305(4)	69(4)
C(21)	1396(7)	3813(8)	1783(4)	60(4)
C(22)	494(8)	4288(10)	1476(5)	98(5)
C(23)	179(9)	5195(11)	1749(6)	135(6)
C(24)	786(10)	5603(10)	2333(5)	132(6)
C(25)	1672(9)	5146(9)	2638(5)	100(6)
C(26)	1984(8)	4261(8)	2374(4)	77(4)
C(31)	4165(6)	−133(7)	1171(4)	39(3)
C(32)	5137(6)	−475(7)	1252(4)	49(3)
C(33)	5345(7)	−1530(7)	1194(4)	62(4)
C(34)	4600(7)	−2259(8)	1052(4)	68(4)
C(35)	3623(7)	−1936(8)	976(5)	76(4)
C(36)	3412(6)	−880(8)	1043(4)	57(4)
C(41)	5015(5)	1944(7)	1394(4)	41(3)
C(42)	5509(6)	2331(8)	2028(4)	60(4)
C(43)	6463(7)	2804(9)	2139(5)	79(5)
C(44)	6915(7)	2890(8)	1641(5)	78(4)
C(45)	6436(7)	2518(8)	1002(5)	71(4)
C(46)	5492(6)	2040(8)	875(4)	57(4)

[a] The equivalent isotropic Gaussian parameter *U*(eq) is $^1/_3\sum r_i^2$ ($i = 1-3$), where r_i's are the root-mean-square amplitudes of the AGDP's (anisotropic Gaussian displacement parameters).

Table 8. Selected Interatomic Lengths (Å) for **15**

Rh−P(2)	2.203(2)	C−O	1.068(11)
Rh−N	2.146(6)	P(2)−C(2)	1.836(7)
Rh−C	1.918(11)	P(2)−C(31)	1.825(8)
Rh−Cl	2.402(2)	P(2)−C(41)	1.811(7)
N−Si	1.720(7)	Si−C(7)	1.857(9)
P(1)−N	1.584(5)	Si−C(8)	1.841(9)
P(1)−C(l)	1.809(7)	Si−C(9)	1.862(9)
P(1)−C(11)	1.786(8)	C(1)−C(2)	1.406(9)
P(1)−C(21)	1.802(9)		

Table 9. Selected Interatomic Angles (deg) for **15**

C−Rh−N	178.3(3)	P(2)−C(2)−C(3)	117.8(6)
C−Rh−P(2)	92.3(2)	P(2)−C(31)−C(32)	123.6(7)
Cl−Rh−C	87.5(2)	P(2)−C(31)−C(36)	118.4(6)
Cl−Rh−N	92.2(2)	P(2)−C(41)−C(42)	125.1(7)
Cl−Rh−P(2)	176.9(1)	P(2)−C(41)−C(46)	116.9(5)
P(2)−Rh−N	88.1(2)	P(1)−C(1)−C(2)	122.9(6)
Rh−N−P(1)	109.9(4)	P(1)−C(1)−C(6)	118.5(6)
Rh−C−O	177.7(7)	P(1)−C(11)−C(12)	122.7(5)
Rh−N−Si	118.2(4)	P(1)−C(11)−C(16)	119.5(7)
Rh−P(2)−C(2)	116.7(2)	P(1)−C(21)−C(22)	120.0(7)
Rh−P(2)−C(31)	115.4(2)	P(1)−C(21)−C(26)	122.0(7)
Rh−P(2)−C(41)	113.8(3)	C(2)−P(2)−C(31)	100.9(4)
P(1)−N−Si	131.9(5)	C(2)−P(2)−C(41)	104.7(3)
N−P(1)−C(11)	111.0(4)	C(31)−P(2)−C(41)	103.6(4)
N−P(1)−C(21)	112.1(4)	C(1)−P(1)−C(21)	105.7(4)
N−P(1)−C(1)	115.0(4)	C(1)−P(1)−C(11)	105.6(4)
N−Si−C(7)	109.9(4)	C(11)−P(1)−C(21)	106.9(4)
N−Si−C(8)	110.0(4)	C(7)−Si−C(8)	108.1(5)
N−Si−C(9)	111.5(4)	C(7)−Si−C(9)	106.3(5)
P(2)−C(2)−C(1)	123.3(5)	C(8)−Si−C(9)	110.9(5)

A comparison of bond lengths about the rhodium center and the carbonyl infrared stretching frequencies is summarized in Table 10. Although the compounds listed in the table are not all chelate complexes with the same ring size as **15**, the bond lengths are remarkably similar except for the rhodium−carbonyl linkage. The Rh−C bond in **15** is longer by approximately 0.1 Å and the C−O bond is shorter by 0.1 Å compared to the others (**19**−**24**) listed in Table 10. Closer examination of Figure 2 suggests an explanation because it is clear that the ellipsoid representing the carbonyl carbon is elongated and oriented along the rhodium−carbonyl axis. The structure is therefore slightly disordered and we suggest that the system represents another example of a "displacement disorder"[35] which might arise in this case from the presence of a small amount of the *trans* carbonyl−P(III) complex in the crystal. This would interchange the carbonyl and chloride ligands in the structure without altering the positions of rest of the ligand atoms. A small percentage of the *trans* isomer would be sufficient to significantly alter the Rh−C bond length because of the much greater X-ray diffracting power of chlorine (17 electrons) over carbon (6 electrons)[35] so we do not ascribe any unusual bonding interactions to the apparently anomalous distance. We did not however detect this *trans* species by spectroscopic analysis of the complex in solution, so it may be an artifact of the particular crystal selected.

The most striking feature of the structure of **15** is the P═N−Si bond angle of 131.9(5)°. This angle has decreased 21° from 152.7(3)° in the free ligand **2** as a result of coordination of the nitrogen lone pair of electrons to the rhodium center. Both the P═N and N−Si bonds also lengthen noticeably upon complex formation from 1.529(5) and 1.672(5) Å respectively in **2** to 1.584(5) and 1.720(7) Å in **15**. Similarly, the P−N−Si angle decreases and the P═N and N−Si bonds lengthen upon complexation of Ph_3P═N−$SiMe_3$ with CuCl.[36] The changing bond lengths and angles further support the view that the bonding in the uncomplexed P═N−Si linkage reflects delocalized bond contraction and strengthening through the diffusion of the lone pair of electrons on nitrogen into orbitals on phosphorus and silicon, and while the older calculations suggested d-orbital participation as the responsible factor, other more recent assessments[24,37−39] suggest that the $\pi-\sigma^*$ negative

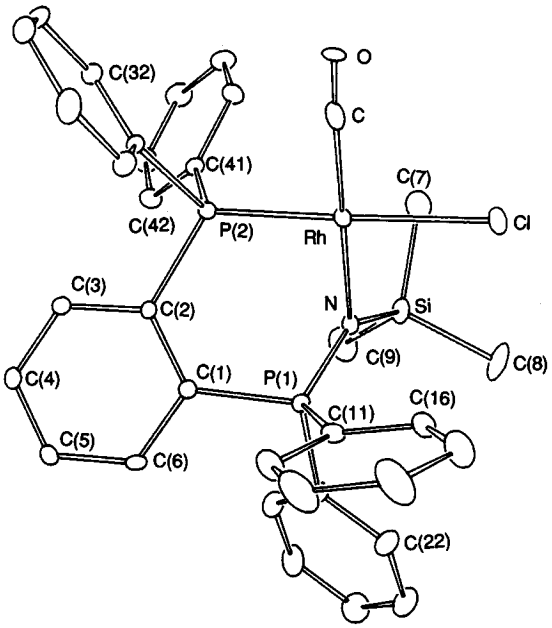

Figure 2. Representation of the molecular structure of **15** showing the atom numbering scheme. Atoms are shown as Gaussian ellipsoids at the 20% probability level.

Table 10. Structural and IR (Carbonyl) Data for Rhodium Complexes

	bond lengths (Å)					ν_{CO}
complex	Rh−P	Rh−Cl	Rh−C	C−O	Rh−N	(cm^{-1})
15[a]	2.203(2)	2.402(2)	1.918(11)	1.068(11)	2.146(6)	1980
19[b]	2.156(1)	2.384(1)	1.815(3)	1.141(5)	2.199(2)	1991
20[c]	2.261(2)		1.786(9)	1.155(11)	2.098(9)	
21[d]	2.322	2.381(2)	1.800(2)	1.150(7)		
22[e]	2.326	2.371(2)	1.810(7)	1.144(8)		1980
23[f]	2.230(3)	2.410	1.78(1)	1.12(1)		1986
24[g]	2.232(1)		1.809(6)	1.145		

[a] This work. [b] Bondoux, D.; Mentzen, B. F.; Tkatchenko, I. *Inorg. Chem.* **1981**, *20*, 839. [c] Liepoldt, J. G.; Basson, S. S.; Dennis, C. R. *Inorg. Chim. Acta* **1981**, *50*, 121. [d] Monge, A.; Gutièrrez-Puebla, E.; Herase, J. V.; Pinilla, E. *Acta. Crystallogr. Sect. C* **1983**, *C39*, 446. [e] Bonnet, J. J.; Jeannin, Y.; Kalck, P.; Maisonnat, A.; Poilblanc, R. *Inorg. Chem.* **1975**, *14*, 743. [f] Ceriotti, A.; Ciani, G.; Sironi, A. *J. Organomet. Chem.* **1983**, *247*, 345. [g] Leipoldt, J. G.; Grobler, E. C. *Inorg. Chim. Acta* **1982**, *60*, 141.

hyperconjugation model is more appropriate. Coordination interferes with the delocalization of the lone pair of the nitrogen towards phosphorus and silicon which is responsible for the larger angles and shorter bond lengths in the free silylated ligands and so the ligands with silyl groups distort from a planar trigonal toward a linear geometry. The directional donation of the lone pair of the sp^2 nitrogen in formation of the complexes restores the trigonal planar geometry at the nitrogen center.

The bond angle in **15** is similar to that demonstrated by the oxodiphenoxyphosphoranimine complex $(PhO)_2P(O)$-N═$PPh_2N(Et)Ph_2PRh(CO)Cl$[2](120.7° with a P═N distance of 2.21Å)[2] where the backbone is an amine and in the fluoroaromatic complex, 4-CNC_6F_4N═$PPh_2CH_2Ph_2PRh(CO)Cl$[5] (where this same angle is 113.2° and the P═N distance is 1.616 Å)[5]. In this latter case the backbone is a CH_2 group.

Conclusion

The rigid backbone of *cis*-bis(phosphines) limits the Staudinger oxidation of such compounds to one of the two phosphorus

(35) See for example: Yoon, K.; Parkin, G.; Rheingold, A. L. *J. Am. Chem. Soc.* **1991**, *113*, 1437.
(36) Fenske, D.; Böhm, E.; Dehnicke, K.; Strähle, J. *Z. Naturforsch., B* **1988**, *43B*, 1.
(37) Reed, A. E.; Schleyer, P. R. *J. Am. Chem. Soc.* **1990**, *112*, 1434.
(38) Gilheany, D. G. *Chem. Rev.* **1994**, *94*, 1339.
(39) Messmer, R. P. *J. Am. Chem. Soc.* **1991**, *113*, 433.

centers thus producing an asymmetric (iminophosphorano)-phosphine. The inhibition of oxidation results from the effects of steric congestion on the azide reaction process because the phosphorus centers related by a *cis* conformation on a rigid backbone cannot form the necessary Staudinger intermediate in the second stage of the process. This steric effect was demonstrated by the oxidation of only one phosphorus center in 1,2-bis(diphenylphosphino)benzene and in *cis*-1,2-bis(diphenylphosphino)ethylene. The facile reaction of both phosphorus centers in *trans*-1,2-bis(diphenylphosphino)ethylene rules out electronic effects of an unsaturated backbone as the responsible factor. The structure of **2** and theoretical examination of the P═N−Si linkage reveals that much shorter bond lengths and larger bond angles are to be expected in silyliminophosphines compared to the P═N−C linkage of phosphinimines containing an organic substituent as a result of the delocalization of the electron density on nitrogen into phosphorus and silicon based orbitals. Complexation of the imine center reverses the delocalization of the electron density on nitrogen and reestablishes the trigonal planar geometry expected at nitrogen. The asymmetric (iminophosphorano)phosphines prepared herein are good complexing agents forming chelated square-planar Rh(I) complexes through the phosphine and imine nitrogen donor centers.

Experimental Section

All of the synthetic work was carried out using standard Schlenk techniques. All solvents were distilled prior to their use and all reactions were carried out under an argon atmosphere. NMR spectra were recorded on Bruker WP200 [^{1}H (200.133 MHz), ^{13}C (50.323 MHz), and ^{31}P (81.015 MHz)], Bruker AM300 [^{1}H(300.13 MHz), ^{13}C (75.469 MHz)], and Bruker WH400 [^{1}H (400.135 MHz), ^{13}C (100.614 MHz), ^{19}F (376.503 MHz), ^{29}Si (79.495 MHz) and ^{31}P (161.978 MHz)] instruments in CD_2Cl_2 or $CDCl_3$ solvents which were also used for the instrumental lock. All shifts are quoted relative to tetramethylsilane (for ^{1}H, ^{13}C, and ^{29}Si) and 85% H_3PO_4 for ^{31}P. Positive shifts lie downfield in all cases. Infrared spectra were recorded as CH_2Cl_2 casts on KBr cells on a Nicolet FTIR spectrometer. Low resolution EI mass spectra were recorded on a AEI MS12 magnetic sector mess spectrometer at 70 eV (sometimes 16 eV). Chemical analyses were performed by the Microanalytical Laboratory, Chemistry Department, University of Alberta. Melting points were obtained on a MEL-TEMP melting point apparatus and were uncorrected.

Total Synthesis of 1,2-Bis(diphenylphosphino)benzene (1). ***Caution!*** The intermediate diphenyl(trimethylsilyl)phosphine used in this procedure is deceptively pyrophoric with an indeterminate induction period. The phosphine can be pipetted and weighed into an open, argon-filled flask, but contact with paper or tissue will invariably cause a fire. *This might not occur for several minutes!*

Bromoiodobenzene was first prepared from 2-bromoaniline[16] as a brown-red liquid in 56% yield and isolated by vacuum distillation 65−68 °C (0.6 mmHg). Anal. Calcd: C, 25.34; H, 1.40%. Found: C, 25.47; H, 1.43. Next, diphenyltrimethylsilylphosphine was then prepared from triphenylphosphine and trimethylsilyl chloride via lithiation of the triphenyl phosphine.[16] Double distillation produced 40 g (155 mmol, 81%) of Ph_2PSiMe_3 as a clear, colorless liquid, bp 110−115 °C (0.02 mmHg), lit.[16] 119−120 °C (0.2 mmHg). ^{31}P NMR: −55.9 ppm; lit.[16] −56.2 ppm. In the next step, (2-bromophenyl)diphenylphosphine was prepared from Ph_2PSiMe_3 in a catalyzed reaction with a small amount of $PdCl_2(PhCN)_2$ (250 mg, 0.65 mmol) to give a tan-colored solid, (2-bromophenyl)diphenylphosphine, mp 105−108 °C, lit.[16] 112−114 °C. ^{31}P NMR: −4.0 ppm; lit.[16] −4.4 ppm. Finally, 1,2-bis(diphenylphosphino)benzene[16] **(1)** was prepared as follows: Into a 250 mL side arm round-bottom flask was placed 2.40 g (7.04 mmol) of (2-bromophenyl)diphenylphosphine and 100 mL of dry THF. The solution was then cooled to −78 °C and 5 mL of 1.6 M nBuLi was added dropwise. The solution was then stirred for 1 h before the slow addition of 1.60 g (7.27 mmol) of chlorodiphenylphosphine in 20 mL of THF. The solution was stirred overnight and allowed to warm to room temperature slowly. The solvent was removed using a rotary evaporator to produce a thick oil, which was dissolved in 50 mL of hot 50/50 ethanol/toluene. Gravity filtration through a fluted filter paper and slow cooling to room temperature produced 2.00 g (4.48 mmol, 64%) of **1** as small white crystals, mp 176−179 °C, lit.[16] 179−181 °C. ^{31}P NMR: −12.8 ppm; lit.[16] −14.2 ppm.

Reaction of 1 with Azides. With Trimethylsilyl Azide: Formation of 2. Into a 250 mL 24/40 round bottom flask was placed 9.86 g (22.1 mmol) of **1**, 3.03 g (26.3 mmol) of trimethylsilyl azide,[17] and 100 mL of dry toluene. The flask was fitted with a water-cooled reflux condensor, and the solution was refluxed vigorously. The progress of the reaction was monitored by ^{31}P NMR spectroscopy, and more azide was added periodically. After 5 days of heating, the cooled solution was filtered under argon to remove some fluffy precipitate, and the flask was placed in the freezer (−20 °C) overnight. Filtration of the cold solution under argon produced 6.80 g (12.8 mmol, 58%) of pure **2** as small white crystals, mp 165−169 °C. Anal. Calcd for $C_{33}H_{33}P_2NSi$: C, 74.27; H, 6.23; N, 2.62. Found: C, 74.28; H, 6.36; N, 2.65. IR (CH_2Cl_2 cast): 3053 s, 2949 s, 1580 m, 1568 w, 1550 w, 1481 s, 1435 vs, 1305 br vs, 1265 w, 1239 m, 1177 w, 1110 s, 1067 w, 1022 m, 995 w, 906 w, 859 vs, 828 vs, 744 vs, 712 s, 695 vs, 650 w, 580 w, 540 vs, 513 m, 495 w. MS: M^+, 533 (2%), 456 (100%). ^{1}H NMR (δ, $CDCl_3$, TMS): 7.6−7.2 ppm, m, 24H; 0.04 ppm, s, 9H. ^{31}P NMR (δ, $CDCl_3$, H_3PO_4): 1.23 ppm, d; −14.77 ppm, d, $^3J_{PP}$ = 17.8 Hz. ^{13}C NMR (δ, $CDCl_3$, TMS): 139−127 ppm, Ar; 5.58 ppm, $^3J_{CP}$ = 3.0 Hz. ^{29}Si NMR (δ, $CDCl_3$, TMS): −12.06 ppm, $^2J_{SiP}$ = 20.7 Hz.

With 4-Cyanotetrafluorophenyl Azide: Formation of 3. To a chloroform solution (30 mL) of **1** (1.81 g, 4.05 mmol) at 0 °C was added dropwise 0.95 g (4.40 mmol) of 4-$CNC_6F_4N_3$[22] in 20 mL of chloroform. The reaction was complete in 1 h as determined by ^{31}P NMR spectroscopy. The reaction mixture was stirred overnight, and then the solvent was removed *in vacuo*. Recrystallization from acetonitrile produced 2.20 g (3.47 mmol, 86%) of fine, off-white crystals of **3**, mp 211−213 °C. Anal. Calcd for $C_{37}H_{24}F_4P_2N_2$: C, 70.04; H, 3.81; N, 4.41. Found: C, 69.84; H, 4.02; N, 4.26. IR (CH_2Cl_2 cast): 3055 w, 2225 w, 1647 m, 1502 s, 1433 m, 1230 m, 1103 w, 1050 s br, 980 s, 739 w, 734 m, 715 m, 690 s, 528 vs, 511 w, 505 w, 492 m. MS: M^+, 634 (23%), 557 (100%). ^{1}H NMR (δ, $CDCl_3$, TMS): 8.0−7.0 ppm, Ar. ^{31}P NMR (δ, $CDCl_3$, H_3PO_4): 11.88 ppm, dt, $^3J_{PP}$ = 21.0 Hz, $^4J_{PF}$ = 4.54 Hz; −14.84 ppm, d, $^3J_{PP}$ = 20.8 Hz. ^{19}F NMR (δ, $CDCl_3$, C_6F_6): −139.4 ppm, m; −151.7 ppm, m.

With Diphenoxyphosphoryl Azide: Formation of 4. Into a 100 mL 24/40 round bottom flask were placed 3.00 g (6.72 mmol) of **1**, 1.85 g (6.72 mmol) of diphenoxyphosphoryl azide (Aldrich), and 50 mL of dry toluene. The reaction mixture was stirred and heated gently overnight. Removal of the solvent *in vacuo*, followed by repeated addition of CH_2Cl_2 to the resulting oil and removal of the solvent *in vacuo* eventually produced an off-white, hydroscopic, amorphous powder, mp 56 °C. Anal. Calcd for $C_{42}H_{34}O_3P_3N$: C, 72.73; H, 4.94; N, 2.02. Found: C, 72.43; H, 5.22; N, 1.95. IR (CH_2Cl_2 cast): 3075 w, 2970 w, 1594 m, 1489 s, 1435 m, 1304 m br, 1244 m, 1203 br vs, 1162 w, 1114 m, 1026 w, 913 s, 746 s, 718 w, 691 s, 536 s, 497 m. MS: M^+, 693 (1%), 616 (5%). ^{1}H NMR (δ, $CDCl_3$, TMS): 7.8−6.7 ppm, Ar. ^{31}P NMR (δ, $CDCl_3$, H_3PO_4): 13.8 ppm, dd, $^3J_{PP}$ = 23.6 Hz; −8.9 ppm, d, $^2J_{PP}$ = 36.2 Hz; −15.9 ppm, d, $^3J_{PP}$ = 23.6 Hz.

With Benzyl Azide: Formation of 5. Into a Schlenk tube were placed 5 g (20 mmol of azide) of Amberlite anion exchange resin (chloride replaced by azide),[25] 1.00 g (5.85 mmol) of benzyl bromide, and enough CH_2Cl_2 to saturate the resin (20 mL). This mixture was stirred for 8 h at room temperature. The solution was then filtered under argon and the resin was washed with two 10-mL portions of CH_2Cl_2. (***Caution!*** This is potentially dangerous! Exposure of the azide to a glass frit could cause detonation of the azide.) The CH_2Cl_2 solution containing the azide was then added dropwise to a CH_2Cl_2 solution (20 mL) of **1** (2.33 g, 5.22 mmol) at 0 °C. The reaction mixture was allowed to warm slowly overnight, and removal of the solvent *in vacuo* produced an oil. Dissolving the oil in a minimum of CH_2Cl_2 and the addition of 100 mL of dry hexane produced an oil. The solvent was decanted from the oil and both fractions were analyzed by ^{31}P NMR spectroscopy. The solvent fraction contained **5** exclusively, but the oil contained a large variety of unknown phosphorus-containing compounds. The solvent fraction was recrystallized from acetonitrile

to yield approximately 1 g (30%) of pure **5**, mp 129−131 °C. Anal. Calcd for $C_{37}H_{31}P_2N$: C, 80.57; H, 5.66; N, 2.54. Found: C, 80.19; H, 5.68; N, 2.98. Calcd with 0.2 mol of acetonitrile: C, 80.24; H, 5.69; N, 3.00. IR (CH_2Cl_2 cast): 3050 w, 2800 w, 2120 (CH_3CN), 1585 w, 1490 w, 1480 m, 1437 s, 1280 m br, 1182 m, 1108 s, 1026 m, 998 w, 724 s br, 694 vs, 548 m, 530 m. MS: $M^+ - 77$, 474 (100%). ^{1}H NMR (δ, $CDCl_3$, TMS): 7.8−6.9 ppm, Ar, 29H; 4.5 ppm, d, $^3J_{HP}$ = 16.97 Hz; (1.97 ppm CH_3CN). ^{31}P NMR (δ, $CDCl_3$, H_3PO_4): 10.3 ppm, d, $^3J_{PP}$ = 15.0 Hz; −13.9 ppm, d, $^3J_{PP}$ = 15.5 Hz. ^{13}C NMR (δ, $CDCl_3$, TMS): 138−125 ppm, Ar; 49.75 ppm, s.

Complexes with $[Rh(CO)_2Cl]_2$. Complex with 2: Formation of 15. A CH_2Cl_2 solution (30 mL) of **2** (0.2884 g, 0.5411 mmol) was added dropwise to a CH_2Cl_2 solution (80 mL) of $[Rh(CO)_2Cl]_2$ (0.1029 g, 0.2645 mmol)[40] at room temperature. After 1 h the initial red solution had turned yellow-orange and the solvent was removed *in vacuo*. Phosphorus NMR spectroscopy of the resulting yellow microcrystalline powder revealed a clean conversion to complex **15**. Recrystallization from 25 mL of hot acetonitrile produced large clear orange blocks of **15** (59 mg, 0.84 mmol, 16%), mp 255 °C (discolored), 264 °C (decomposed−degassed vigorously). Anal. Calcd for $C_{34}H_{33}P_2NSiRhOCl$: C, 58.34; H, 4.75; N, 2.00. Found: C, 57.72; H, 4.77; N, 2.18. IR (CH_2Cl_2 cast): 3050 w, 2940 w, 2890 w, 1980 vs, 1580 w br, 1435 m, 1240 w, 1139 m, 1126 s, 1107 w, 1093 m, 835 s, 769 m, 750 w, 743 w, 727 m, 693 s, 581 m, 555 s, 542 m, 507 m. MS: $M^+ - CO$, 671 (87.5%). ^{1}H NMR (δ, $CDCl_3$, TMS): 7.7−7.2 ppm, Ar, 24H; −0.29, s, 9H. ^{31}P NMR (δ, $CDCl_3$, H_3PO_4) 40.45, dd, $^1J_{PRh}$ = 175.2 Hz, $^3J_{PP}$ = 19.1 Hz; 20.16, dd, $^3J_{PP}$ = 19.2 ppm, $^2J_{PRh}$ = 1.86 Hz. ^{13}C NMR (δ, $CDCl_3$, TMS): carbonyl not observed, 137−127 ppm, Ar; 5.60 ppm, $^3J_{CP}$ = 4.16 Hz. ^{29}Si NMR (δ, $CDCl_3$, TMS): 6.6 ppm, d, $^2J_{SiP}$ = 5.08 Hz.

Complex with 3: Formation of 16. A CH_2Cl_2 solution (20 mL) of **3** (0.1616 g, 0.255 mmol) was added dropwise to a CH_2Cl_2 solution (30 mL) of $[Rh(CO)_2Cl]_2$ (0.0496 g, 0.127 mmol)[40] at room temperature. The next day the initial red solution had turned yellow-orange and the solvent was removed *in vacuo*. Phosphorus NMR spectroscopy of the resulting yellow microcrystalline powder revealed quantitative formation of complex **16**. Recrystallization from 50 mL of hot acetonitrile produced small yellow cubes (100 mg, 0.14 mmol, 55%) of **16**, mp 312 °C dec. Anal. Calcd for $C_{38}H_{24}F_4P_2N_2OClRh$: C, 56.99; H, 3.02; N, 3.50. Found: C, 56.50; H, 2.85; N, 3.50. IR (CH_2Cl_2 cast): 2930 w, 2240 w, 1986 vs, 1643 m, 1493 s, 1484 s, 1435 m, 1184 m, 1113 m, 997 w, 981 m, 892 w, 741 m, 729 m, 581 m, 529 m. MS: $M^+ - 35$ 675 (1%); $M^+ - 35 - 28$, 737 (4%); $M^+ - 35 - 28 - 77$, 660 (8%); M, 28 (100%). ^{1}H NMR (δ, $CDCl_3$, TMS): 7.8−7.2 ppm, m, Ar. ^{31}P NMR (δ, $CDCl_3$, H_3PO_4): 36.52 ppm, dd, $^1J_{PRh}$ = 169.6 Hz, $^3J_{PP}$ = 27.86 Hz; 27.84, d, broad. ^{19}F NMR (δ, $CDCl_3$, C_6F_6): −137.5, m; −142.5, m.

Complex with 4: Formation of 16. A CH_2Cl_2 solution (50 mL) of **4** (0.1493 g, 0.215 mmol) was added dropwise to a CH_2Cl_2 solution (50 mL) of $[Rh(CO)_2Cl]_2$ (0.0419 g, 0.216 mmol)[40] at −78 °C. The solution was allowed to warm slowly to room temperature and the solvent was removed *in vacuo*. Phosphorus NMR spectroscopy of the resulting yellow microcrystalline powder revealed clean formation of the complex **16**, mp 116 °C dec. Anal. Calcd for $C_{43}H_{34}P_3O_4NClRh$: C, 60.05; H, 3.98; N, 7.63. Found: C, 57.82; H, 3.97; N, 7.75. IR (CH_2Cl_2 cast): 3057 w, 1986 vs, 1590 m, 1489 s, 1436 m, 1261 m br, 1195 m, 1120 s, 1097 m, 10265 w, 930 s, 810 m, 746 m, 690 s, 553 m, 513 m. ^{1}H NMR (δ, $CDCl_3$, TMS): 8.0−7.0 ppm, Ar. ^{31}P NMR (δ, $CDCl_3$, H_3PO_4): 50.0 ppm, dd, $^1J_{PRh}$ = 170.6 Hz, $^3J_{PP}$ = 20.1 Hz; 40.5 ppm, overlapping dd; 7.3 ppm, d, $^2J_{PP}$ = 18.49 Hz. ^{13}C NMR (δ, $CDCl_3$, TMS): 185.9 ppm, dd, $^1J_{CRh}$ = 78.5 Hz, $^2J_{CP}$ = 16.1 Hz; 151 ppm, d, J = 7.0 Hz, 137−120 ppm, Ar.

Reaction of 10 with 4-$NCC_6F_4N_3$. To a cold (−78 °C) methylene chloride solution (approximately 75 mL) of **10** (1.05 g, 2.65 mmol)[21] was added dropwise 0.58 g (2.7 mmol) of 4-NC-C_6F_4-N_3 [22] in approximately 25 mL of methylene chloride. Upon completion of the addition, the dry ice/acetone cooling bath was removed and the reaction mixture was allowed to warm to room temperature and stirred overnight. A 5 mL aliquot was removed, and the ^{1}H and ^{31}P NMR spectra were recorded. The solvent was removed *in vacuo*, and the residue was recrystallized from 30 mL of hot acetonitrile, producing 1.05 g (1.80 mmol, 68%)) of **12** as pale yellow crystals, mp 111−114 °C. Anal. Calcd for $C_{33}H_{22}F_4N_2P_2$: C, 67.81; H, 3.79; N, 4.79. Found: C, 66.78; H, 4.03; N, 4.91. IR (CH_2Cl_2 cast): 3050 w, 2229 m, 1644 s, 1502 vs, 1436 s, 1222 s, 1112 m, 1011 m, 999 m, 981 s, 742 m, 720 s, 708 m, 694 s, 563 m. MS: M^+, 584 (14%), 507 (100%). ^{1}H NMR (δ, $CDCl_3$, TMS): 7.9−7.1 ppm, m, Ar. ^{31}P NMR (d, $CDCl_3$, H_3PO_4): 0.16 ppm, −25.65 ppm, $^3J_{PP}$ = 12.5 Hz, $^4J_{PF}$ = 5.5 Hz, $^7J_{PF}$ = 6.5 Hz.

Reaction of 11 with 4-$NCC_6F_4N_3$. To a cold (−78 °C) methylene chloride solution (approximately 75 mL) of **11** (1.05 g, 2.65 mmol) was added dropwise 0.60 g (2.8 mmol) of 4-$NCC_6F_4N_3$ in approximately 25 mL of methylene chloride. Upon completion of the addition, the dry ice/acetone cooling bath was removed, and the reaction mixture was allowed to warm to room temperature and stirred overnight. A 10 mL aliquot was removed, and the ^{1}H and ^{31}P NMR spectra were recorded. ^{31}P NMR data for **13** (P(III) −4.42 ppm, $^3J_{PP}$ = 15.3 Hz; P(V) 7.84 ppm, $^4J_{PF}$ = 5.2 Hz); for **14** (P(III) −23.7 ppm, $^3J_{PP}$ = 12.5 Hz, $^4J_{PF}$ = 5.5Hz; P(V) 2.06 ppm, $^3J_{PP}$ = 12.5 Hz, $^7J_{PF}$ = 6.7 Hz).

Complexation of 12 with $[Rh(CO)_2Cl]_2$: Formation of 18. A 10 mL solution of **12** (0.1159 g, 0.198 mmol) was added dropwise at room temperature to a 15 mL solution of $[Rh(CO)_2Cl]_2$ (0.0390 g, 0.100 mmol). The mixture was stirred for 1 h before the solvent was removed *in vacuo* and the resultant yellow-orange solution analyzed by ^{31}P NMR spectroscopy. Slow recrystallization from methylene chloride/diethyl ether produced crystals of **18**, mp 160 °C dec. Anal. Calcd for $C_{34}H_{22}F_4N_2P_2RhOCl$: C, 54.38; H, 2.95; N, 3.73. Found: C, 53.65; H, 2.71; N, 3.73. IR (CH_2Cl_2 cast): 3060 w, 2980 w, 2241 m, 1989 vs, 1643 s, 1493 s, 1485 s, 1435 m, 1181 m, 1113 m, 1099 m, 1003 m, 998 m, 982 m, 895 m, 739 m, 730 m, 716 m, 693 m, 674 w, 627 w, 588 m, 559 w, 509 w. ^{1}H NMR (δ, CD_2Cl_2, TMS): 7.9−7.2 ppm, m, Ar. ^{31}P NMR (d, CD_2Cl_2, H_3PO_4): P(III) 29.73 ppm, $^1J_{PRh}$ = 171.0 Hz, $^3J_{PP}$ = 37.4 Hz; P(V) 15.24 ppm, $^3J_{PP}$ = 37.6 Hz. ^{13}C NMR (d, CD_2Cl_2, TMS): carbonyl ligand 186.8 ppm, $^1J_{CRh}$ = 72.5 Hz, $^2J_{CP}$ = 19.6 Hz.

Acknowledgment. We thank the Natural Sciences and Engineering Research Council of Canada and the University of Alberta for support. We also thank Mr. Rod Gagne for synthetic assistance

Supporting Information Available: For **2**, tables of crystallographic experimental data (Table S1-1), interatomic distances (Table S1-2), interatomic angles (Table S1-3), weighted least-squares planes (Table S1-4), torsional angles (Table S1-5), atomic coordinates and anisotropic gaussian displacement parameters (Table S1-6), hydrogen atom coordinates and isotropic Gaussian displacement parameters (Table S1-7), atomic coordinates and equivalent isotropic Gaussian parameters. anisotropic and equivalent isotropic Gaussian displacement parameters (Table S1-9), and root-mean-square amplitudes of anisotropic Gaussian displacement parameters (Table S1-10), and for **15**, tables of crystallographic experimental data (Table S2-1), interatomic lengths (Table S2-2), interatomic angles (Table S2-3), weighted least-squares planes (Table S2-4), torsional angles (Table S2-5), atomic coordinates and anisotropic Gaussian displacement parameters (Table S2-6), hydrogen atom coordinates and isotropic Gaussian parameters (Table S2-7), atomic coordinates and equivalent isotropic Gaussian parameters (Table S2-8), anisotropic and equivalent isotropic Gaussian displacement parameters (Table S2-9), and root-mean-square amplitudes of anisotropic Gaussian displacement parameters (Table S2-10) (23 pages). Ordering information is given on any current masthead page.

(40) McCleverty, J. A.; Wilkinson, G. *Inorg. Synth.* **1990**, *28*, 84.

IC9514713